

## MUON GUIDE MADE OF UNITS OF MAGNETIZED IRON

G. B. Bondarenko\*, V. A. Glukhikh\*\*, Yu. P. Dobretzov\*, B. A. Dolgoshein\*, V. A. Kantzerov\*, A. V. Kiselev, V. G. Kirillov-Ugryumov\*, A. V. Samoylov, Yu. M. Sapunov, R. M. Sulyaev, V. A. Titov\*\*, A. M. Frolov, I. A. Shukevlo\*\*

Institute for High Energy Physics, Serpukhov, USSR.

\*) Moscow Physical-Engineering Institute, Moscow, USSR.

\*\*\*) D. V. Efremov Scientific Investigation Institute for Electro-physical Apparatus, Moscow, USSR.

### 1. Introduction

A number of experimental physical problems at accelerators requires detection of high energy muons, produced far from the detector. As muons weakly interact with the substance, then magnetized iron appears to be good to keep muons effectively in a considerably small area close to the required direction and to transport them at a considerable distance. The muon guide, described below, was designed for the experiment on studying processes of muon production in NN collisions, in particular, to search for intermediate bosons at the IHEP accelerator. According to the experimental requirements, the muon guide was to provide measurements of muon energy spectra in the energy range 10-30 GeV as well as measurements of the muon slowing down to a stop, the purpose of which is muon polarization over symmetry of  $\mu$ -e decay. Besides it was necessary to have a large acceptance of the muon guide with minimum losses of muons along the path.

### 2. Design and Layout

The equipment layout in the experimental hall is presented in Fig. 1. The muon guide consists of three sections: the head objective, a bending magnet, and the end objective. The head objective is made of 4 steel cylinders, situated on the beam axis. The current that goes along the cylinder axis is homogeneously distributed through its cross section and excites axial-symmetrical induction  $B = \frac{1}{2} \mu j r$  in the cylinder. Here  $j$  is the cur-

rent density,  $\mu$  is the magnetic permeability of the steel,  $r$  is the radius of the coaxial layer in the cylinder. Depending on the charge sign of the particle and the current direction, the cylinder operates either as a focusing or a defocusing lens. In this, as distinguished from ordinary quadrupole lenses, focusing is performed in all the planes. A general view of the steel lens is given in Fig. 2; Fig. 3a illustrates experimental radial distributions of the induction inside the lenses at various values of the current going through it. The lenses of the end objective are similar to the ones already described, 10 bending magnets (Fig. 4) deflect the muon beam to the experimental set-up. The operational induction in the magnet is established over the hysteresis loop, presented in Fig. 3b. Technical characteristics of the lenses and the magnets are listed in Table I. Free spaces between the units of the muon guide were chosen proceeding from the location of particle detectors. Units of each of the three sections are fed in series.

The Monte-Carlo method was used in designing the muon guide, taking into account experimental measurements on induction, multicoulomb scattering and fluctuations in ionization losses of energy. According to the calculated data, the muon guide captures muons with energies up to 33 GeV in the angular range  $\pm 1.5^\circ$  and holds about 60% of captured particles along the corresponding lengths of the path, determined by energy losses up to the values of order of straggling.

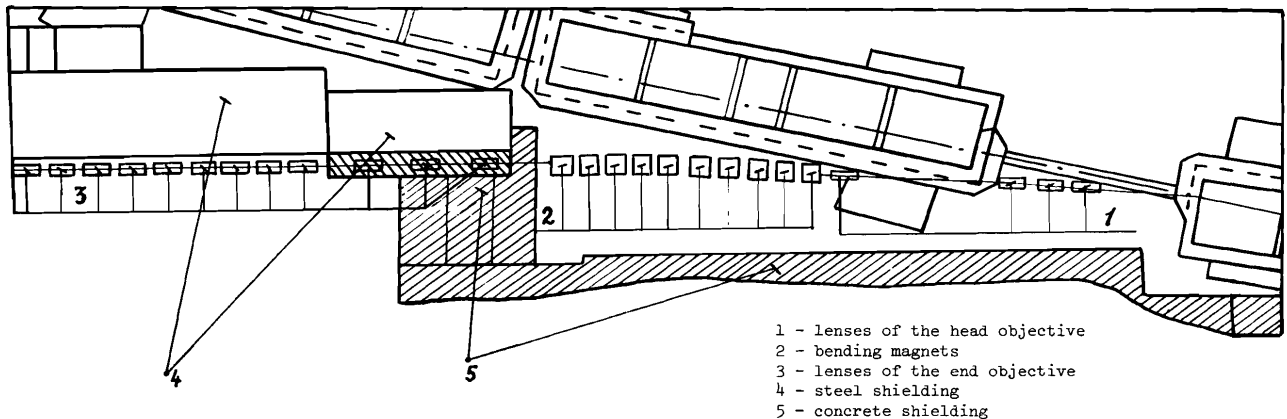


Fig. 1: The layout of the equipment for the muon guide in the experimental area of the IHEP accelerator.

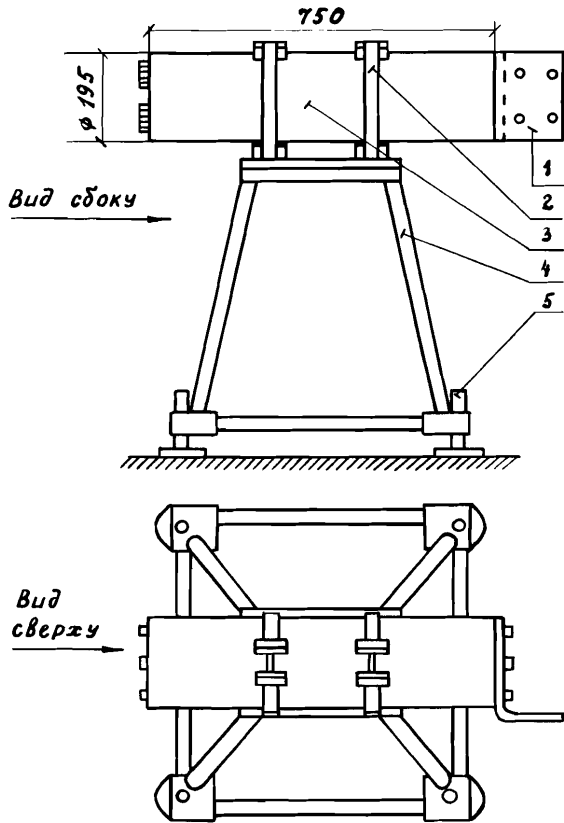


Fig. 2: General view of the muon lens  
 1 - current supply; 2 - holder; 3 - lens;  
 4 - support; 5 - jack.

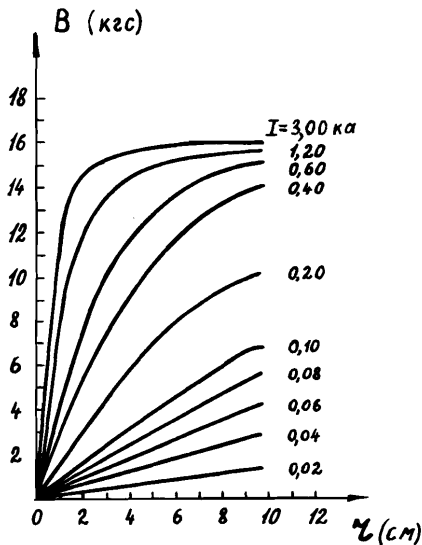


Fig. 3a: Radial distributions of induction B at different values of the full current, I.

Fig. 5 presents a number of experimental curves that illustrate the focusing properties of the head objective. The curves present muon fluxes in the relative units at different cross sections of the muon guide, through which pass particles with the energy higher than some other, that is determined by the amount of the material in front of the cross section. It can be explained by the fact that at high energies of muons, the later ones travel a long way until stopped and there is a high probability of their being knocked out from the muon guide because of multiple scattering and initial beam divergence. For example, for muons with energy above 16 GeV, focusing by the head objective provides for a particle flux mu-factor of 16; in the case of muons with  $E > 12$  GeV it is the same as the case when the head objective is off.

Fig. 6 presents another set of experimental curves that illustrate analysing properties of the muon guide (Fig. 6a) and focusing properties of the end objective (6b). Each of the curves in Fig. 6b was obtained at values of the induction in the bending magnets that provide the maximum muon flux of the corresponding energy.

Analysis of the experimental data shows that at optimum operational modes of the lenses of the head and end objectives, the muon guide provides an intensity of muons some 20 to 40 times higher than that with non-magnetized iron, equivalent over the amount of material, along the path of the muon beam. It should also be noticed that the lenses of the muon guide also analyse particles according to the charge sign. For example, when remagnetizing the lenses of the end objective the count of particles at the end of the muon guide dropped down to zero.

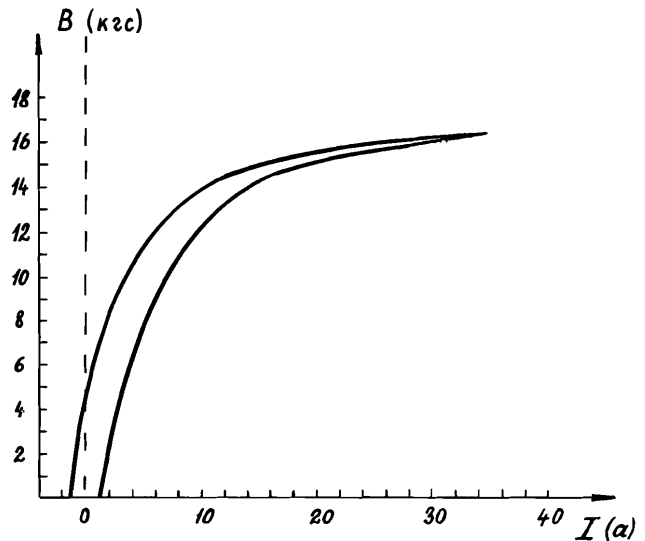


Fig. 3b: Hysteresis curve of the bending magnet

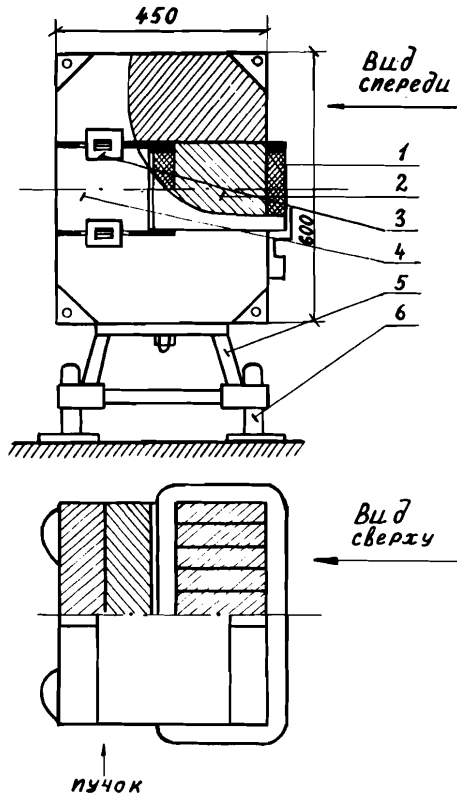


Fig. 4: General view of the bending magnets  
 1 - winding; 2 - body; 3 - measuring gap;  
 4 - support; 5 - jack.

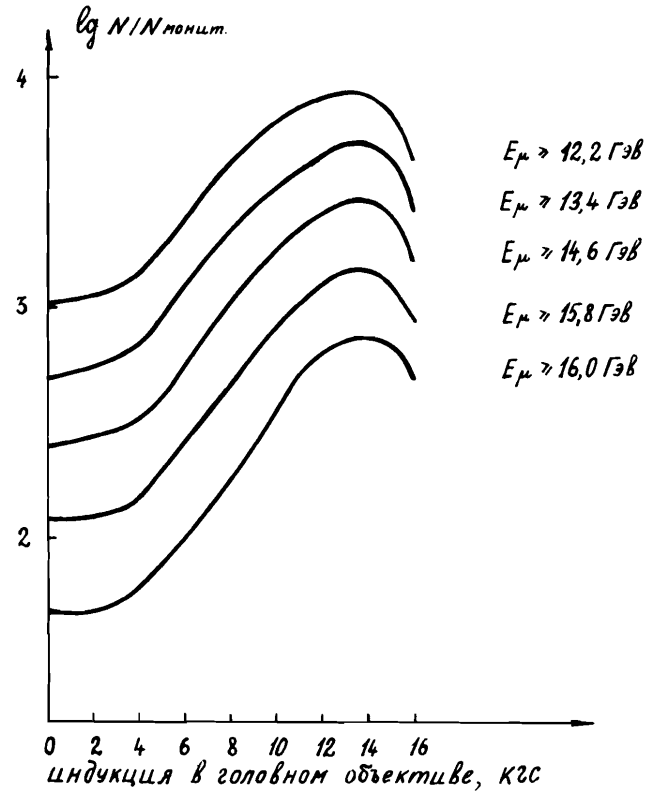


Fig. 5: Focusing properties of the head objective of the muon beam for an induction in the bending magnets of 10 kG and an induction at the aperture edge of the lenses of the end objective of 14 kG ( $N/N_{\text{monit}}$  = relative particle flux).

Table I - Technical Characteristics of the Muon Lenses and Magnets

Characteristics	Lens	Magnet
Dimensions (width x height x length)	19.5 cm x 95 cm	50 x 60 x 60 cm <sup>3</sup>
Dimensions of the operational aperture (width x height x length)	19.5 cm x 75 cm	20 x 20 x 50 cm <sup>3</sup>
Weight	250 kg	1070 kg
Current	2000 A	9.5 A
Voltage drop	0.007 V	3.5 V
Induction	15 kG on the edge	13 kG
Induction nonhomogeneities in the experimental area	-	1%

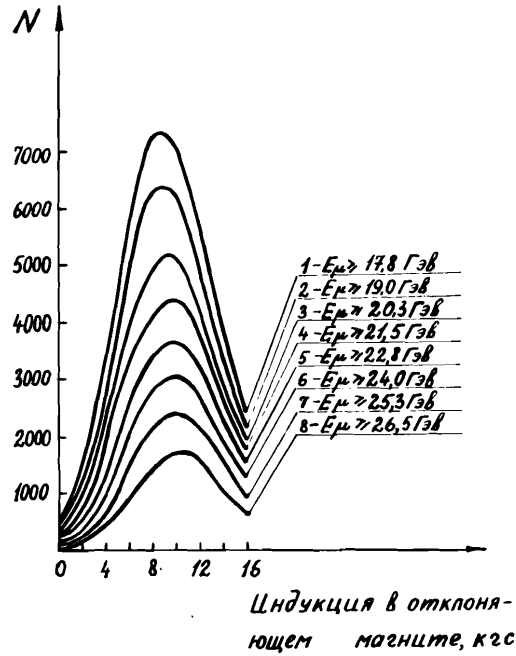


Fig. 6a: Analysing properties of the bending magnets of the muon beam at an induction at aperture edge of the head and the end objectives of 10 kG and 12 kG, respectively.

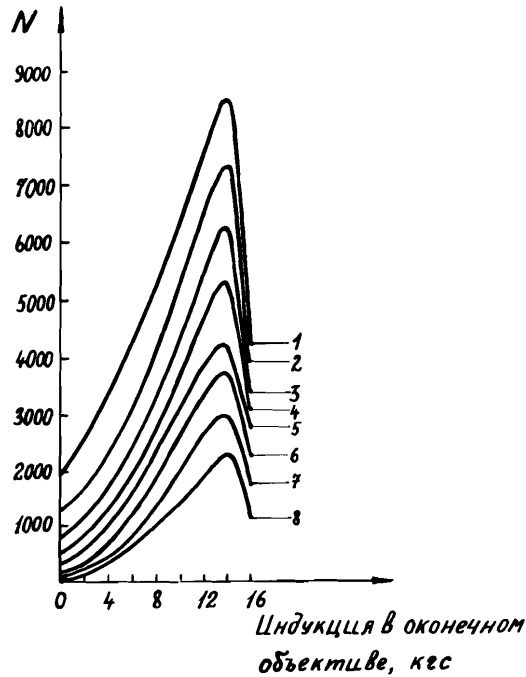


Fig. 6b: Focusing properties of the end objective of the muon beam at an induction at the edge of the aperture of the lenses in the head objective of 10 kG and an induction at the bending magnets optimum over the particle flux on the curves (Fig. 6a) ( $N$  is the particle flux in relative units).

